

Article

# Manufacture of 2D-Printed Precision Drug-Loaded Orodispersible Film Prepared from Tamarind Seed Gum Substrate

Kampanart Huanbutta <sup>1</sup>, Pornsak Sriamornsak <sup>2</sup>, Inderbir Singh <sup>3</sup> and Tanikan Sangnim <sup>1,\*</sup>

- <sup>1</sup> Faculty of Pharmaceutical Sciences, Burapha University, 169, Saensook, Muang, Chonburi 20131, Thailand; kampanart@go.buu.ac.th
- <sup>2</sup> Department of Pharmaceutical Technology, Faculty of Pharmacy, Silpakorn University, Nakorn Pathom 73000, Thailand; sriamornsak\_p@su.ac.th
- <sup>3</sup> Chitkara College of Pharmacy, Chitkara University, Patiala 140401, Punjab, India; inderbir.singh@chitkara.edu.in
- \* Correspondence: tanikan@go.buu.ac.th

**Abstract:** Two-dimensional (2D) printing is a simple technology that shows the possibility for the preparation of personalized pharmaceutical dosage forms. This technology can accurately print medicine in different sizes, which can be applied to develop a personalized, drug-loaded orodispersible film for patients with dysphagia. Seed gum from *Tamarindus indica* Linn was selected as the film former of the printing substrate, and sorbitol was applied as a film plasticizer. Theophylline was used as a printed model drug due to its narrow therapeutic index. From the results, the mechanical properties of the film indicated that increasing the level of sorbitol improved the flexibility and strength of the film, which rendered the gum film suitable as a printing substrate. Conversely, raising portions of the gum (more than 3.5%) led to the use of rigid and stress-resistant films that can crack during the printing process. The Fourier transform infrared result revealed that there was no interaction between theophylline and the gum after the printing process. The printed theophylline was mainly in an amorphous form based on the X-ray diffraction results. Furthermore, theophylline was deposited at the surface of the gum substrate after the drug-printing process, as depicted in the scanning electron microscope images. The printed drug on the orodispersible film can be accurately determined by varying the printing size/repeat. Lastly, the drug was completely released from the orodispersible film within 5 min. The research results showed the possibility of utilizing tamarind seed gum as a potential printing substrate for the 2D drug-printing technique. Moreover, this can be applied as an electronic prescribing system for telemedicine in the future.



**Citation:** Huanbutta, K.; Sriamornsak, P.; Singh, I.; Sangnim, T. Manufacture of 2D-Printed Precision Drug-Loaded Orodispersible Film Prepared from Tamarind Seed Gum Substrate. *Appl. Sci.* **2021**, *11*, 5852. <https://doi.org/10.3390/app11135852>

Academic Editor: Greta Varchi

Received: 30 April 2021  
Accepted: 22 June 2021  
Published: 24 June 2021

**Publisher's Note:** MDPI stays neutral with regard to jurisdictional claims in published maps and institutional affiliations.



**Copyright:** © 2021 by the authors. Licensee MDPI, Basel, Switzerland. This article is an open access article distributed under the terms and conditions of the Creative Commons Attribution (CC BY) license (<https://creativecommons.org/licenses/by/4.0/>).

**Keywords:** elderly; orodispersible film; personalized medicine; precision medicine; two-dimensional printing technology

## 1. Introduction

Drug production technology in the 21st century tends to be personalized [1,2] to reduce the risk of adverse drug reactions and to optimize therapeutic efficiency; accordingly, two-dimensional (2D) printing technology has been adapted to manufacture orodispersible films. This is because 2D printing can digitally deposit a very small amount of drug (ink) on a substrate (edible carrier) [3]. Among several 2D printing techniques, inkjet printing has been applied for manufacturing drug-loaded films due to its feasibility and the high precision/accuracy of the deposited ink volume. Therefore, inkjet printing technology is a suitable method for film preparation prior to loading high-potency and/or narrow therapeutic index drugs [4,5]. Two-dimensional printing techniques are also precise methods that could be implemented in a hospital setting in the future for the preparation of personalized doses [6]. Ink (drug solution/suspension) properties, including viscosity, surface tension, boiling temperature, and solvent evaporation rate, play a vital role in the

quality of the printing process [7]. Moreover, flexible and highly absorbent properties are required to effectively print substrates. Therefore, optimizing the formulation of both ink and substrate are necessary to ensure optimum orodispersible film properties.

Orodispersible films are drug-loaded single or multilayer edible sheets that can rapidly dissolve in the mouth. These films can be administered through mastication and water intake because they dissolve in saliva. Orodispersible films are suitable for older adults who generally face problems with psychological dysphagia [8]. Furthermore, they can be administered to both pediatric and psychiatric patients [9]. Orodispersible films can also enhance drug dissolution and absorption owing to drug dispersion throughout the film former [10]. Several methods, such as solvent casting [11], electrospinning [12], and hot-melt extrusion [13], have been applied in the preparation of orodispersible films. However, dose adjustment is a limitation when using orodispersible films prepared using more conventional methods. Thus, inkjet-printing technology has been introduced in order to accurately print adjustable drugs on a film substrate [6]. Two-dimensional printing requires the use of an edible carrier (substrate) that would absorb the deposited ink. HPMC [14], PVA [15], potato starch [4], and rice starch [16] have been used as the substrate for the inkjet drug printing. Most of the substrate polymer has to combine to decrease the contact angle between the ink and the substrate, and enhance the flexibility of the film [17]. In this study, the novel substrate for inkjet printing, which was gum from *Tamarindus indica* seeds, has been introduced due to its hydrophilic and high Young's modulus properties [18].

Due to the numerous advantages of 2D printing, there are groups of studies beginning to apply 2D printing in drug formulation. As an example, Scoutaris et al. used inkjet printing to increase the solubility of a poorly soluble molecule, namely felodipine, with an excipient, namely PVP, to enhance the dispersion property of the controlled release solid dosage form [19]. Additionally, the fabrication of nanoparticle complexes between the BCS class II drugs and the polysaccharide before printing on the substrate provides an abundant scope for progressing the dissolution property of some poorly water-soluble drugs [20]. Inkjet printing is also suitable for low-dose drug formulation. Gaisford et al. showed the application of a simple, home, inkjet printer to print salbutamol films on a paper tray of the printer, which was then modified to print the highest resolution and highest quality drug, provided that the printed templates were designed by Microsoft Word software [4]. From previous studies of a 2D printing application for drug formulation preparation, it could be proven that the drug can be prepared by an inkjet printer. However, the low drug loading is a limitation of this technique. Therefore, the increase in the drug-loading strategy by expanding the printing size and overprinting of a similar area were utilized in this study. To ensure this strategy, the printing accuracy of the loaded drug was testified.

The present investigation was aimed at developing orodispersible films containing drugs and accurately printing them on the tamarind seed gum substrate. The model drug in this study was a narrow therapeutic index drug, namely theophylline [21]. Formulations of the ink (theophylline solution) and the gum-printing substrate were optimized, and the mechanical properties of the printing substrate were assessed. The physical and chemical changes in drug-printed orodispersible films were monitored using a scanning electron microscope (SEM) and a Fourier transform infrared spectrometer (FTIR), respectively. The model drug was printed in different sizes and overprinted many times on the tamarind seed gum substrate. Then, the film disintegration time and the drug dissolution in vitro were also evaluated.

## 2. Materials and Methods

### 2.1. Materials

Crude gum was obtained from *Tamarindus indica* seeds collected from Suratthani province in Thailand. Theophylline (lot No. 00099360-A) was purchased from BASF Thailand. Sorbitol was purchased from Merck. Sodium acetate trihydrate (lot No. 4A432624C) was obtained from Carlo Erba. Potassium di-hydrogen phosphate (lot No. KA391) and

di-sodium hydrogen phosphate anhydrous (lot No. KA621) were received from Kemaus. All other chemicals were of standard pharmaceutical grade.

## 2.2. Preparation of Gum Powder

The tamarind seeds were dried in a hot air oven at 80 °C for 30 min and the seed coat was then peeled off. Then, the dried tamarind endosperm was milled using a hammer mill (Milling Machine, SK 100, RETSCH, Haan, Germany) and passed through a No. 45 sieve (355 µm diameter) [22].

## 2.3. Preparation of the Theophylline Solution (Ink Solution)

A total of 830 mg of theophylline was weighted and then dissolved in 100 mL of purified water. The prepared solution was then sonicated for 15 min to enhance the theophylline solubility. Finally, the theophylline solution was loaded into the printer's ink tank (Piezoelectric inkjet printing, L220, Epson, Suwa, Japan).

## 2.4. Printing Substrate Preparation

The prepared carboxymethylated tamarind gum seed was dissolved in purified water at different concentrations (3.5, 4, 4.5, and 5% *w/w*) and then centrifuged (Centrifuges, Sorvall™ Legend™ X1R, Thermo Scientific, Waltham, MA, USA) at 7000 revolutions/minute for 15 min to remove the precipitate. The sorbitol solution at a concentration of 10% *w/v* was added to the gum solution as a plasticizer at several gum:sorbitol ratios (100:0, 99:1, and 97:3). Then, the gum mixture solution was poured into the mold plate, which was dried in a hot air oven at 60 °C for 18 h. Finally, the dried film (printing substrate) was peeled off the mold plate and kept in a dry cabinet for further investigation and drug printing.

## 2.5. Drug Printing

First, the theophylline solution at a concentration of 5 mg/mL was loaded into the printer's ink tank (Piezoelectric inkjet printing, L220, Epson, Suwa, Japan). The printing resolution was set to 5760 × 1440 dpi, and the target dose was calculated based on the estimated droplet volume, ink concentration, and printing size. The printing substrate was prepared by fixing the gum film onto paper. The drug solution was printed on different surface areas (2 × 2 cm<sup>2</sup>, 4 × 3 cm<sup>2</sup> and 4 × 5 cm<sup>2</sup>). Finally, the theophylline solution was printed 3 to 5 times on the same area to increase the amount of drug deposited on the film.

## 2.6. Assessment of Physicochemical Properties and Morphology of the Printing Substrate

### 2.6.1. Mechanical Properties

The mechanical properties of the prepared gum-printing substrate with/without the loaded drug were evaluated by measuring the tensile strength, percentage of elongation, and Young's modulus using a texture analyzer (TA. XT plus, Stable Micro Systems, Godalming, UK). The substrate was cut to a size of 2 × 2 cm<sup>2</sup>. Then, the substrate was fixed from top to bottom to obtain a gap length of 1 cm. The substrate was then stretched at a rate of 100 mm per minute using a 0.05 N pulling force. The maximum force and pulling length before film breakage was recorded. Then, the tensile strength, percentage of elongation, and Young's modulus were calculated. Each test was repeated 6 times [23].

### 2.6.2. Morphology of the Printing Substrate

The printing substrate morphology was also monitored with scanning electron microscopy techniques (scanning electron microscope (SEM), LEO1450VP, Cambridge, UK). The substrate morphology was observed in both the surface and cross-section views. For the cross-section view sample preparation, the drug-printed substrate was embedded in resin and sliced by the ultramicrotome (Leica Ultracut R, Leica, Wetzlar, Germany). Then both the surface and cross-section samples were pasted onto stubs and sputter coated with gold to increase their conductance.

### 2.6.3. Thickness and Moisture Content of the Printing Substrate

The thickness of the printing substrate was measured using a microprocessor coating thickness gauge. The printing substrate was cut to a size of  $2 \times 2 \text{ cm}^2$  and the thickness was measured 5 times. The moisture content of the printing substrate at  $12 \text{ cm}^2$  (average weight 2 g) was monitored using a moisture sensor (MA 150, Sartorius Weighing Technology GmbH, Goettingen, Germany).

### 2.6.4. Powder X-ray Diffraction

The powder X-ray diffraction (XRD) patterns of the starting materials (theophylline and gum), their physical mixtures, and the drug-printed substrate were obtained using a powder X-ray diffractometer (Model D8, Bruker, Billerica, MA, Germany) under the following conditions: graphite monochromatized  $\text{Cu K}\alpha$  radiation, voltage = 45 kV, electric current = 40 mA, slit:  $\text{DS}1^\circ$ ,  $\text{SS}1^\circ$ , RS 0.15 nm, and scanning ratio  $2\theta = 5^\circ \text{ min}^{-1}$ .

### 2.6.5. Fourier Transform Infrared Spectrometer

The Fourier transform infrared (FTIR) spectra of the starting materials (theophylline and carboxymethylated gum), their physical mixture, and the drug-printed orodispersible films were obtained using the KBr method and an FTIR spectrometer (Magna-IR system 750, Nicolet Biomedical Inc., WI, USA) to investigate the effect of the printing process on the model drug and the gum.

### 2.7. *In Vitro* Disintegration Study

A disintegration test device (Erweka, ZT4, Heusentsamn, Germany) was used to determine the disintegration time of the six orodispersible films cut to a size of  $4 \text{ cm}^2$ . The process involved placing each film onto the tube of the basket rack assembly of the disintegration device without the disc. The disintegration media (distilled water) was maintained at  $37.0 \text{ }^\circ\text{C} \pm 1 \text{ }^\circ\text{C}$  and the time required to completely disintegrate each film was recorded. The disintegration test was conducted in triplicate.

### 2.8. Printed Drug Amount and Drug Content Analysis

To increase the printed drug-loading content on the film, the methods of expansion of printing size and overprinting several times were applied. The drug contents in the orodispersible films at different printing sizes and overprinting repeats, as indicated in Table 1, were determined by dissolving the films in 50 mL of a sodium acetate buffer solution, stirring them for 24 h, and then sonicating them for 2 h before the dispersion was filtered through a  $0.45 \text{ }\mu\text{m}$  cellulose acetate membrane. The amount of theophylline in the filtrate was quantified using high-performance liquid chromatography (Model Agilent 1100 Series HPLC System; Agilent Technologies, Santa Clara, CA, USA) and a C18 column (particle size,  $5 \text{ }\mu\text{m}$ ; diameter, 4.6 mm; length, 25 cm, SGE Analytical Science, Victoria, Australia). The mobile phase was a sodium citrate trihydrate solution [24] and the column effluent was detected at 280 nm using a UV/vis detector. After the results were obtained, the models of relationship between the printing size/repeat and the amount of printed drug were generated. The quantification of the printed drug on the films was performed in triplicate. The percentage of drug content analysis was calculated as presented in the following equation:

$$\text{The drug content analysis (\%)} = \frac{\text{Actual printed drug amount}}{\text{Theoretical printed drug amount}} \times 100$$

**Table 1.** Drug-loading evaluation of the orodispersible films with different printing sizes and overprinting repeat.

Sample No.	Printing Size (cm <sup>2</sup> )	Overprinting Repeat
1	2 × 2	1
2	2 × 2	3
3	2 × 2	5
4	4 × 3	1
5	4 × 5	1

### 2.9. In Vitro Dissolution Study

The dissolution profile of the drug associated with the film was analyzed according to the study methodology proposed by Aliaa N. El Meshad and Arwa S. El, using the dissolution apparatus II (DT 128 light, Erweka, Langen, Germany) [25]. The pH 6.8 phosphate buffer solution, at a volume and temperature of 250 mL and 37 °C ± 0.5 °C, was used as the medium solution. Test fluid (3 mL) samples were taken at various time intervals, i.e., 1, 3, 5, 10, 15, 20, 25, 30, 45, 60, and 120 min. The amount of theophylline released was then analyzed using the HPLC technique (Model Agilent 1100 Series HPLC System; Agilent Technologies, Santa Clara, CA, USA) using a UV/vis detector (280 nm). The types of HPLC column, mobile phase, and theophylline qualification method were similar to those used in the quantification method for the amount of printed drug, as described above [24]. The dissolution test of the film was performed in triplicate.

### 2.10. Statistical Analysis

The analysis of variance (ANOVA) test and Levene's test for homogeneity of variance were performed using SPSS version 10.0 for Windows (SPSS Inc., Chicago, IL, USA). Post hoc testing ( $p < 0.05$ ) of the multiple comparisons was performed by either the Scheffé or Games–Howell test, depending on whether Levene's test for homogeneity was insignificant or significant, respectively.

## 3. Results

### 3.1. Assessment of Physicochemical Properties and Morphology of the Printing Substrate

#### 3.1.1. Mechanical Properties

The film's mechanical properties can be changed by adding sorbitol and altering the concentration of tamarind gum. As presented in Figure 1a, adding sorbitol at 1% and 3% can enhance the mechanical properties of the film. Adding 3% sorbitol, the film tensile strength and elongation percent significantly increased to 96.98 Mpa and 73.66%, respectively. This indicated that the film was resistant and flexible. This may occur because sorbitol strongly interacts with the gum at the molecular level by forming hydrogen bonds with the glucan structure, which is found in tamarind seed gum [26,27]. However, the addition of 5% sorbitol significantly diminished the film strength to 21.37 Mpa because an excessively high proportion of sorbitol hinders inter-polymer bonding. Figure 1b shows that a higher amount of gum (4–5%) in the formulation significantly reduced film stress and strain. This might be due to the low number of H-bonds (in excessive gum proportions), making the film weaker and less flexible [28].

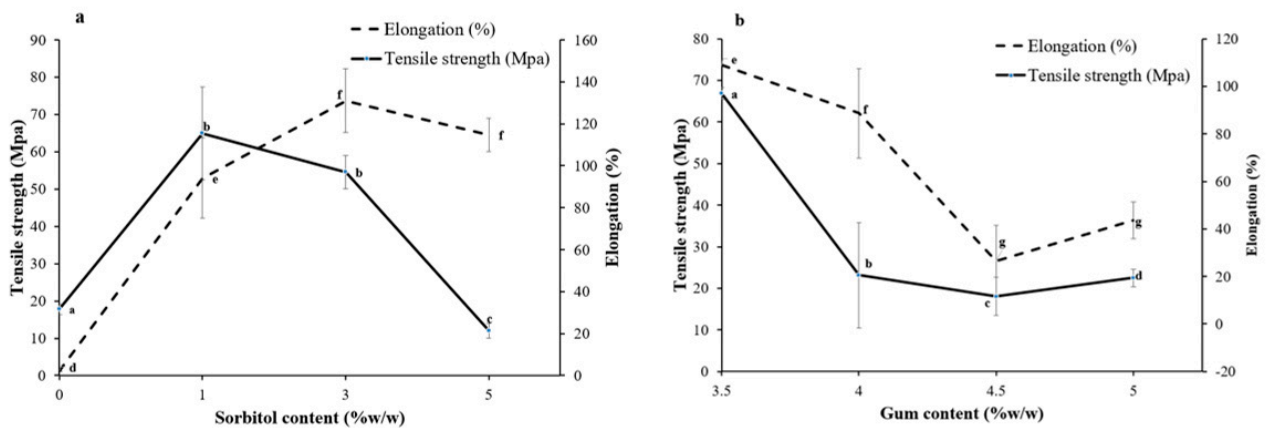


**Figure 1.** Correlation between mechanical properties (stress (dashed line) and strain (solid line)) and portion of (a) sorbitol (gum fixed at 5%) (b) gum (sorbitol fixed at 3%) of the printing substrate (a letter on the graph indicates the level of significance; bars denoted by the same letter are not statistically significant ( $p > 0.05$ )).

The Young's modulus of the gum substrate with different proportions of sorbitol and gum are shown in Figure 2. The addition of sorbitol (1–5%) significantly abated the Young's modulus, as illustrated in Figure 2a. Moreover, the rising gum content in the film formulation slightly lowered the Young's modulus (Figure 2b). These Young's modulus value results are consistent with the results for tensile strength and percent elongation.

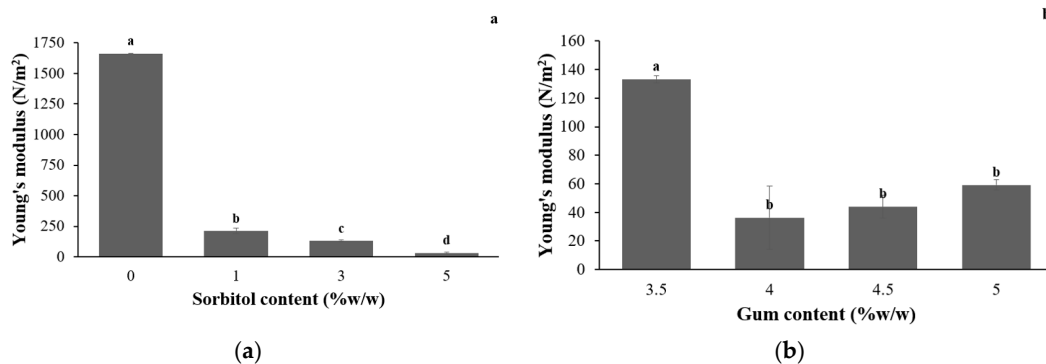


**Figure 2.** Young's modulus of gum substrate at different proportions of (a) sorbitol (gum fixed at 5%) and (b) gum concentration (sorbitol fixed at 3%) (a letter on the bar graph indicates the level of significance; bars denoted by the same letter are not statistically significant ( $p > 0.05$ )).

### 3.1.2. Morphology of the Printing Substrate

According to the film's mechanical properties, the formulation of 3.5% gum and 3% sorbitol was selected for further development of the printing substrate. This is because the selected printing substrate formulation offers high film strength and elasticity, which are required properties for the inkjet-printing process. The surface and cross-section aspects of the blank and drug-printed substrate were monitored by an SEM to reveal the surface morphology of the cast films and the effect of the piezoelectric inkjet printing. The effects of the sorbitol and gum concentration on the morphology of the film were examined and it was determined that the film surfaces were rough, and the sorbitol crystal was not observed in all film formulations of gum and sorbitol at different concentrations, as depicted in Figure 3.

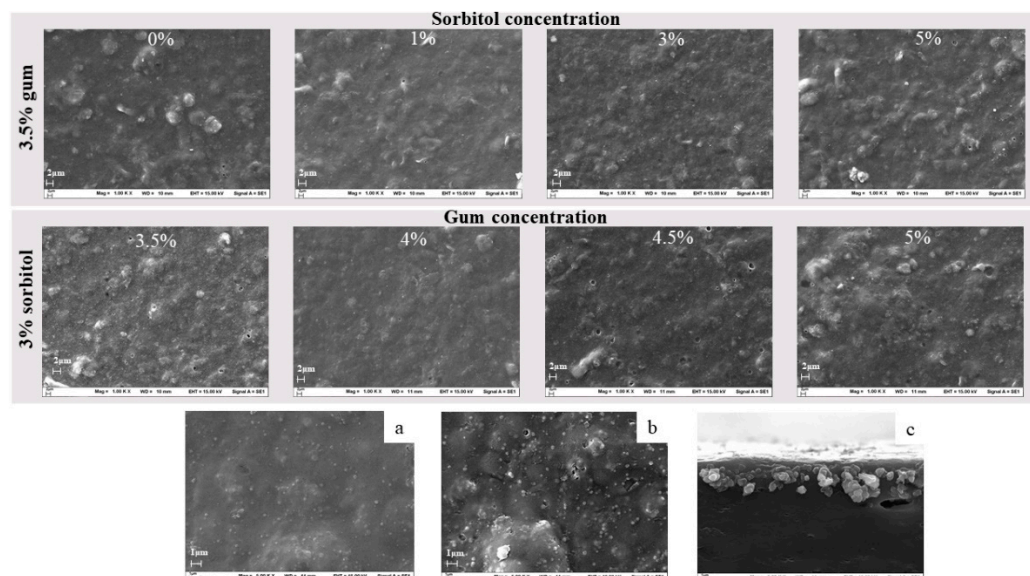


**Figure 3.** Scanning electron microscope images of printing substrates prepared from different concentrations of sorbitol and gum, and also comparison of (a) non-printed, (b) printed substrate surfaces and (c) a cross-sectional view of the printed substrate at 3.5% gum and 3% sorbitol.

The cross section of the drug-printed film and the surface of the printed and non-printed areas were also evaluated using an SEM. There were drug particles on the surface of the printed substrate (Figure 3b) compared to the non-printed area (Figure 3a). The SEM image also shows the deposited theophylline in the form of crystals on the surface of the film substrate and some were absorbed 2  $\mu\text{m}$  deep into the film, as depicted in Figure 3c. This confirms that the drug-printing process was successful. Moreover, the drug absorption in the film could reduce the risk of the API transfer onto the packaging material during storage [29].

### 3.1.3. Thickness and Moisture Content of the Printed Substrate

The thickness and moisture content of the gum film are crucial properties of printing substrates. An adequate printing substrate should be thick enough to resist a bending force during the printing process. However, too thick of a substrate might retard film disintegration. Furthermore, film moisture acts as a plasticizer to improve film flexibility. Nevertheless, too high of a moisture content might affect film stability and ink deposition efficiency [6]. As presented in Table 2, the thickness of the prepared printing substrate was between 106.56  $\mu\text{m}$  and 151.33  $\mu\text{m}$ . The substrate thickness significantly rose when the gum concentration increased. The thickest gum substrate was that of 5% gum and the gum:sorbitol ratio of 97:3. On the other hand, an increment of sorbitol in the formulation did not alter any film thickness.

**Table 2.** Moisture content, film thickness, and disintegration time of different printing substrate formulations.

Gum Concentration (% w/w)	Sorbitol Percent from Gum	Moisture Content (%)	Thickness ( $\mu\text{m}$ )	Disintegration Time (min)
3.5	0	9.30 $\pm$ 1.04	109.11 $\pm$ 23.24	19.31 $\pm$ 0.88
3.5	1	9.29 $\pm$ 0.25	106.56 $\pm$ 30.63	11.16 $\pm$ 1.76
3.5	3	8.31 $\pm$ 0.36	106.89 $\pm$ 10.47	8.14 $\pm$ 0.98
3.5	5	7.49 $\pm$ 0.62	109.11 $\pm$ 18.74	9.33 $\pm$ 0.13
4	3	9.40 $\pm$ 1.12	117.22 $\pm$ 21.28	17.57 $\pm$ 3.24
4.5	3	9.71 $\pm$ 1.57	131.33 $\pm$ 30.71	>30
5	3	9.38 $\pm$ 0.32	151.33 $\pm$ 18.21	>30

Film moisture content ranges from 7.49% to 9.40% as shown in Table 2. An increase in the gum concentration did not affect the moisture content; however, high sorbitol portions lowered the film's moisture content. This result is consistent with a previous study by M.L. Sanyang et al. where they explained that the resemblance of the high molecular structure of glucose units with that of sorbitol caused stronger molecular interactions between the sorbitol and the intermolecular polymer chains. Therefore, the chances of sorbitol interacting with water molecules decreased [30].

#### 3.1.4. Powder X-ray Diffraction

Figure 4 illustrates the powder XRD patterns of the starting materials (gum and theophylline), their physical mixture (PM), the drug-loaded films, and the non-drug-loaded films. Theophylline exhibited characteristic peaks at  $7.14^\circ$ ,  $12.60^\circ$ , and  $14.40^\circ$ , indicating that the theophylline crystals were in monohydrate form [31]. The drug-loaded (printed) films showed halo XRD patterns that were similar to those of the gum and non-drug-loaded films. This demonstrates that the drug on the printed film was in an amorphous form that could enhance the dissolution rate of the theophylline in a neutral-pH medium [32]. Lastly, the XRD pattern of the PM still expressed sharp characteristic peaks that were found in monohydrate theophylline. This reveals that physical mixing cannot alter the drug's crystallinity [33].

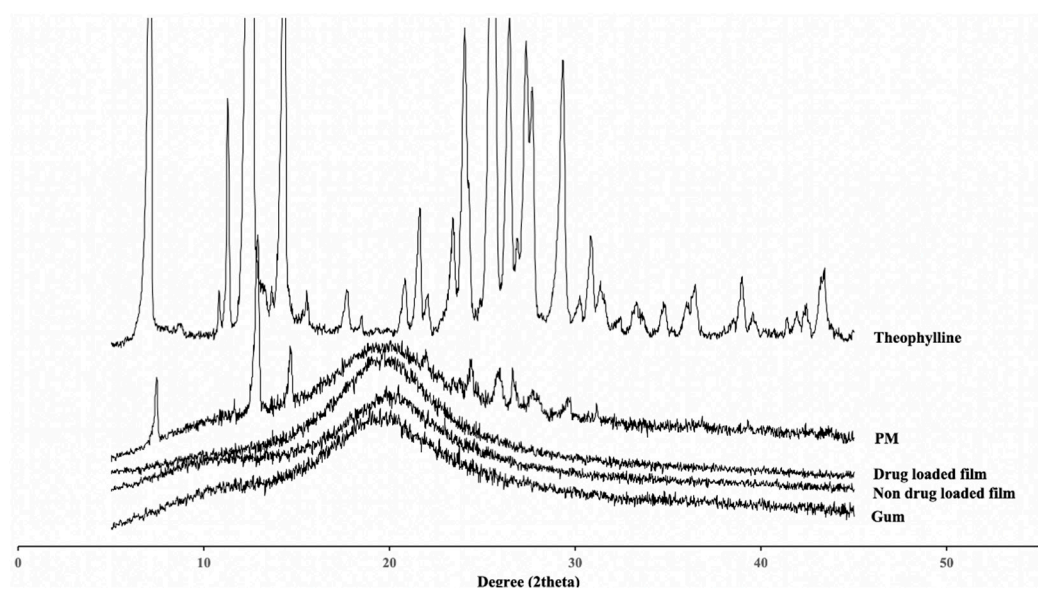


**Figure 4.** Powder XRD patterns of gum, theophylline, their physical mixture (PM), and the drug-loaded/non-drug-loaded films.

#### 3.1.5. Fourier Transform Infrared Spectrometer

The FTIR spectra for theophylline, gum, their physical mixture (PM), and the drug-loaded film are presented in Figure 5. The FTIR spectrum of theophylline showed characteristic peaks at  $3119\text{ cm}^{-1}$  (N–H stretching),  $3063$ ,  $2989$ , and  $2828\text{ cm}^{-1}$  (C–H stretching),  $1718$  and  $1666\text{ cm}^{-1}$  (C=O stretching bands),  $1567$  and  $1443\text{ cm}^{-1}$  (ring stretching),  $1241\text{ cm}^{-1}$  (C–N vibration), and  $1187\text{ cm}^{-1}$  (C–O vibration) [34,35]. The spectrum for the gum expressed major absorption bands associated with a –OH stretching vibration at  $3384\text{ cm}^{-1}$ , and –CH stretching and bending vibrations at  $2924\text{ cm}^{-1}$ , and at approximately  $1410\text{ cm}^{-1}$ , respectively. The absorption band appearing at  $1657\text{ cm}^{-1}$  corresponds to the OH bonds of water molecules [34]. The FTIR spectrum of the physical mixture of the seed gum and theophylline contained important peaks corresponding to the main components. However, the theophylline peaks were rarely observed in the form of drug-printed substrate. This might be because the amount of printed drug was very small compared to that of the gum.

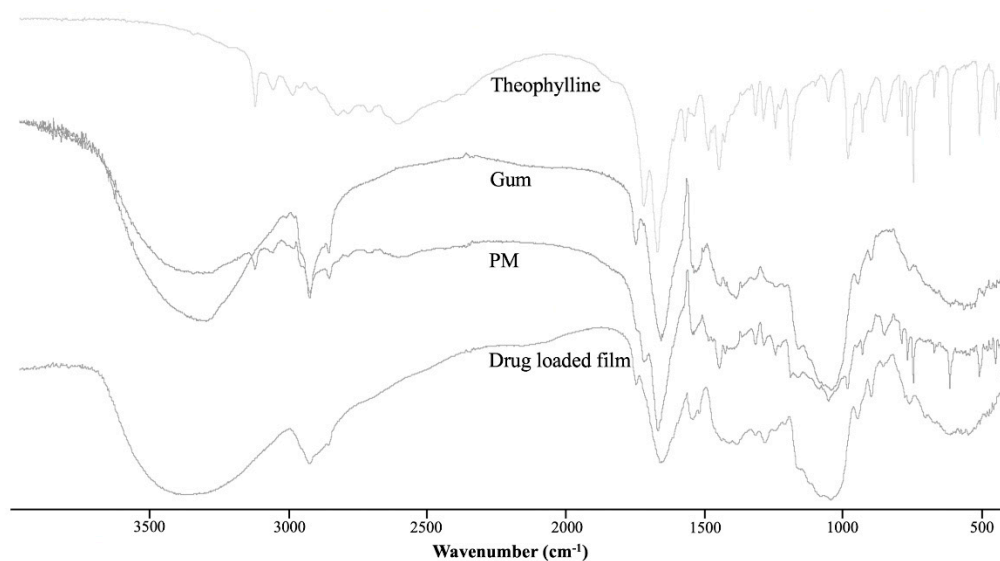


**Figure 5.** FTIR spectra for theophylline, gum, their physical mixture (PM), and the drug-loaded film.

### 3.2. *In Vitro* Disintegration Study

The disintegration times for the orodispersible film, with different concentrations of gum and ratios of sorbitol in the formulation, are presented in Table 2. An increase in the gum concentration extended the disintegration time. Also, adding the film plasticizer (sorbitol) accelerated the film disintegration period. The fastest disintegration lasted 8.14 min, which came from the substrate formulation of the gum concentration of 3.5% and 3% sorbitol from the gum. This might be due to the polyhydroxy groups in the sorbitol molecule increasing the solubility of the film. Sorbitol molecules become inserted between the gum polymer structure, contributing to low-polymer networking and increasing the hydrophilic property of film [26]. The disintegration times of all substrate formulations were longer than 3 min, as indicated in the specifications for oral disintegration tablets of the European pharmacopoeia [36]. This is because the disintegration apparatus is designed for tablet formulations. The sieve size of the disintegration apparatus is narrow, aiming to screen drug particles. Therefore, during the orodispersible film disintegration, the film became a gel, attaching to the screen of the basket of the disintegration apparatus. This made the disintegration time longer. However, the *in vitro* dissolution test result indicated that 77% of the drug was released within 1 min, and 97% of the drug dissolved in 5 min (Figure 6). This result suggests that the disintegration apparatus for orodispersible films must be redesigned, as previously mentioned in the work of Alejandro Rui-Picazo et al. [37]. However, the disintegration time result in this manuscript can be used to compare the solubility of different formulation orodispersible films.

### 3.3. *Printed Drug Amount and Drug Content Analysis*

The amounts of printed drug in various printing sizes and printing replicates are shown in Table 3. The results indicate that a film surface area of 4 cm<sup>2</sup> (2 × 2 cm<sup>2</sup>) contained 28.05 mg of drug. The linear relationship between printed drug content ( $y$ ;  $\mu\text{g}$ ) and printing replicates ( $x$ ) is  $y = 47.98x - 20.86$  with  $r^2$  of 0.9997, and the linear relationship between printed drug content ( $y$ ;  $\mu\text{g}$ ) and printing area ( $x$ ; cm<sup>2</sup>) is  $y = 9.59x - 4$  with  $r^2$  of 0.9800. The drug content analysis percent from the relationship models ranged from 89.72% to 103.42%. From the standard deviation of the drug content analysis, varying the number of printing replicates provided more dose adjustment accuracy. The above can prove that the printed drug can be accurately assigned with a computer program (printing area and replicates).

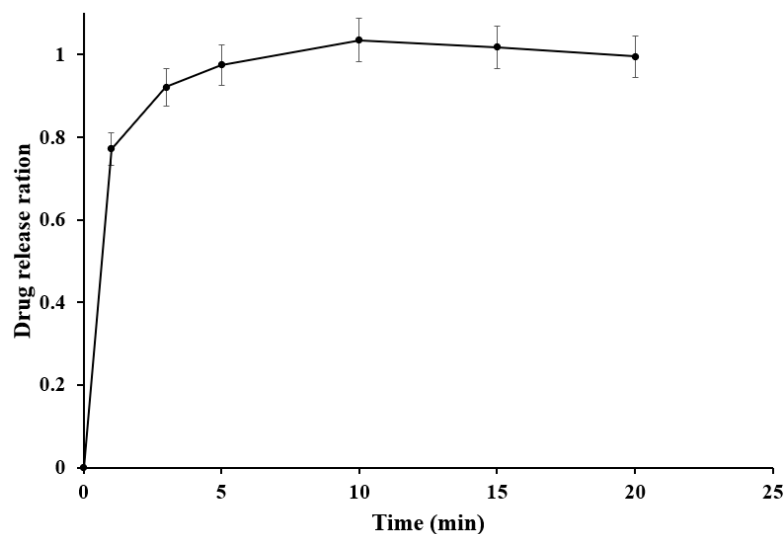


**Figure 6.** Drug dissolution profile for orodispersible film prepared from tamarind seed gum substrate.

**Table 3.** Actual drug content in the prepared orodispersible films and percent of drug content analysis.

Printing Area (cm <sup>2</sup> )	Printing Repeat	Actual Drug Content (µg)	Drug Content Analysis (%)
2 × 2	1	28.05 ± 1.01	96.68 ± 3.47
2 × 2	3	121.21 ± 3.19	101.54 ± 2.67
2 × 2	5	219.97 ± 4.52	99.58 ± 2.04
4 × 3	1	123.80 ± 5.21	89.72 ± 3.77
4 × 5	1	181.58 ± 6.65	103.42 ± 3.78

### 3.4. In Vitro Dissolution Study

As presented in Figure 6, the drug was immediately released in the first minute (77.12%). Then, drug dissolution reached 97.52% at the fifth minute. The in vitro dissolution time was shorter than the film disintegration time because most of the theophylline was dispersed/deposited on the gum film, as presented in the SEM images, which can enhance drug dissolution. Moreover, the film was very thin, resulting in quick swelling and dissolution. However, the printing substrate stuck to the bottom of the fine-pore sieve of the disintegration tester, leading to a delay in the disintegration time result. This result is in agreement with previous work from Pedro M. Castro and coworkers, which reported that the guar gum film prepared from a solvent-casting technique abruptly dissolved in the medium with the help of sorbitol as a plasticizer [38].

## 4. Conclusions

This study demonstrates that the gum from the tamarind seed in the appropriate concentration (3.5%), together with an adequate plasticizer (sorbitol), has the potential to become a printing substrate for the 2D drug-printing manufacture of orodispersible films. The formulated gum substrate can be printed without cracking or the printing becoming stuck. Piezoelectric inkjet printing can deposit theophylline on the surface and at a 2 µm depth from the gum substrate. The accurate amount of drug can be delivered to the printing substrate by varying the printing size and replicates. Theophylline completely dissolved within 5 min from the optimized orodispersible films. This 2D drug-printing manufacturing system of orodispersible films can be developed for personalized dosage forms for pediatric and geriatric use. Moreover, ordering 2D drug printing remotely can be applied to telepharmacy.

**Author Contributions:** Conceptualization, T.S.; methodology, K.H.; supervision, P.S. and I.S.; writing—original draft, K.H.; writing—review and editing, T.S. All authors have read and agreed to the published version of the manuscript.

**Funding:** This research was funded by Faculty of Pharmaceutical Science, Burapha University, grant number Rx10/2564.

**Institutional Review Board Statement:** Not applicable.

**Informed Consent Statement:** Not applicable.

**Acknowledgments:** The study has been funded by the faculty of pharmaceutical sciences, Burapha University.

**Conflicts of Interest:** The authors declare no conflict of interest.

## References

1. Issa, A.M. Personalized medicine and the practice of medicine in the 21st century. *McGill J. Med.* **2007**, *10*, 53.
2. Vaz, V.M.; Kumar, L. 3D Printing as a Promising Tool in Personalized Medicine. *AAPS PharmSciTech* **2021**, *22*, 1–20. [[CrossRef](#)] [[PubMed](#)]
3. Musazzi, U.M.; Khalid, G.M.; Selmin, F.; Minghetti, P.; Cilirzo, F. Trends in the production methods of orodispersible films. *Int. J. Pharm.* **2020**, *576*, 118963. [[CrossRef](#)]
4. Buanz, A.B.M.; Saunders, M.H.; Basit, A.W.; Gaisford, S. Preparation of personalized-dose salbutamol sulphate oral films with thermal ink-jet printing. *Pharm. Res.* **2011**, *28*, 2386–2392. [[CrossRef](#)] [[PubMed](#)]
5. Vuddanda, P.R.; Alomari, M.; Dodoo, C.C.; Trenfield, S.J.; Velaga, S.; Basit, A.W.; Gaisford, S. Personalisation of warfarin therapy using thermal ink-jet printing. *Eur. J. Pharm. Sci.* **2018**, *117*, 80–87. [[CrossRef](#)] [[PubMed](#)]
6. Öblom, H.; Sjöholm, E.; Rautamo, M.; Sandler, N. Towards printed pediatric medicines in hospital pharmacies: Comparison of 2D and 3D-printed orodispersible warfarin films with conventional oral powders in unit dose sachets. *Pharmaceutics* **2019**, *11*, 334. [[CrossRef](#)]
7. Gans, B.D.; Duineveld, P.C.; Schubert, U.S. Inkjet printing of polymers: State of the art and future developments. *Adv. Mater.* **2004**, *16*, 203–213. [[CrossRef](#)]
8. Slavkova, M.; Breitzkreutz, J. Orodispersible drug formulations for children and elderly. *Eur. J. Pharm. Sci.* **2015**, *75*, 2–9. [[CrossRef](#)]
9. Scarpa, M.; Stegemann, S.; Hsiao, W.-K.; Pichler, H.; Gaisford, S.; Bresciani, M.; Paudel, A.; Orlu, M. Orodispersible films: Towards drug delivery in special populations. *Int. J. Pharm.* **2017**, *523*, 327–335. [[CrossRef](#)]
10. El-Setouhy, D.A.; Abd El-Malak, N.S. Formulation of a novel tianeptine sodium orodispersible film. *AAPS PharmSciTech* **2010**, *11*, 1018–1025. [[CrossRef](#)] [[PubMed](#)]
11. Dinge, A.; Nagarsenker, M. Formulation and evaluation of fast dissolving films for delivery of triclosan to the oral cavity. *AAPS PharmSciTech* **2008**, *9*, 349–356. [[CrossRef](#)]
12. Vasvári, G.; Kalmár, J.; Veres, P.; Vecsernyés, M.; Bácskay, I.; Fehér, P.; Ujhelyi, Z.; Haimhoffer, Á.; Rusznyák, Á.; Fenyvesi, F. Matrix systems for oral drug delivery: Formulations and drug release. *Drug Discov. Today Technol.* **2018**, *27*, 71–80. [[CrossRef](#)]
13. Jani, R.; Patel, D. Hot melt extrusion: An industrially feasible approach for casting orodispersible film. *Asian J. Pharm. Sci.* **2015**, *10*, 292–305. [[CrossRef](#)]
14. Steiner, D.; Finke, J.H.; Kwade, A. SOFTs—Structured orodispersible film templates. *Eur. J. Pharm. Biopharm.* **2019**, *137*, 209–217. [[CrossRef](#)]
15. Buanz, A.B.; Belaunde, C.C.; Soutari, N.; Tuleu, C.; Gul, M.O.; Gaisford, S. Ink-jet printing versus solvent casting to prepare oral films: Effect on mechanical properties and physical stability. *Int. J. Pharm.* **2015**, *494*, 611–618. [[CrossRef](#)] [[PubMed](#)]
16. Wickström, H.; Nyman, J.O.; Indola, M.; Sundelin, H.; Kronberg, L.; Preis, M.; Rantanen, J.; Sandler, N. Colorimetry as quality control tool for individual inkjet-printed pediatric formulations. *AAPS PharmSciTech* **2017**, *18*, 293–302. [[CrossRef](#)] [[PubMed](#)]
17. Azizi Machekposhti, S.; Mohaved, S.; Narayan, R.J. Inkjet dispensing technologies: Recent advances for novel drug discovery. *Expert Opin. Drug Discov.* **2019**, *14*, 101–113. [[CrossRef](#)] [[PubMed](#)]
18. SantoshNaidu, M.; Radha, G.; Girish, P.; Lohithasu, D. Comparison studies on transdermal films of natural tamarind seed polysaccharide extract containing anti hypertension drug with PVA. *HPMC Guar Gum World J. Pharm. Res.* **2014**, *3*, 753–763.
19. Scoutaris, N.; Ross, S.; Douroumis, D. Current trends on medical and pharmaceutical applications of inkjet printing technology. *Pharm. Res.* **2016**, *33*, 1799–1816. [[CrossRef](#)]
20. Cheow, W.S.; Kiew, T.Y.; Hadinoto, K. Combining inkjet printing and amorphous nanonization to prepare personalized dosage forms of poorly-soluble drugs. *Eur. J. Pharm. Biopharm.* **2015**, *96*, 314–321. [[CrossRef](#)]
21. Jonkman, J.H.G. Therapeutic consequences of drug interactions with theophylline pharmacokinetics. *J. Allergy Clin. Immunol.* **1986**, *78*, 736–742. [[CrossRef](#)]
22. Huanbutta, K.; Sangnim, T.; Sittikijyothin, W. Development of tamarind seed gum as dry binder in formulation of diclofenac sodium tablets. *Walailak J. Sci. Technol.* **2016**, *13*, 863–874.
23. Bin Liew, K.; Tan, Y.T.F.; Peh, K.K. Characterization of oral disintegrating film containing donepezil for Alzheimer disease. *AAPS PharmSciTech* **2012**, *13*, 134–142. [[CrossRef](#)]
24. The National Formulary, USP 40 NF. 2017. Available online: <https://search.library.wisc.edu/catalog/999509774402121> (accessed on 12 January 2021).

25. El Meshad, A.N.; El Hagrasy, A.S. Characterization and optimization of orodispersible mosapride film formulations. *AAPS PharmSciTech* **2011**, *12*, 1384–1392. [[CrossRef](#)]
26. Antoniou, J.; Liu, F.; Majeed, H.; Qazi, H.J.; Zhong, F. Physicochemical and thermomechanical characterization of tara gum edible films: Effect of polyols as plasticizers. *Carbohydr. Polym.* **2014**, *111*, 359–365. [[CrossRef](#)] [[PubMed](#)]
27. Huanbutta, K.; Sittikijyothin, W.; Sangnim, T. Development of topical natural based film forming system loaded propolis from stingless bees for wound healing application. *J. Pharm. Investig.* **2020**, *50*, 625–634. [[CrossRef](#)]
28. Shaw, N.B.; Monahan, F.J.; O’riordan, E.D.; O’sullivan, M. Physical properties of WPI films plasticized with glycerol, xylitol, or sorbitol. *J. Food Sci.* **2002**, *67*, 164–167. [[CrossRef](#)]
29. Buanz, A.B.; Telford, R.; Scowen, I.J.; Gaisford, S. Rapid preparation of pharmaceutical co-crystals with thermal ink-jet printing. *CrystEngComm* **2013**, *15*, 1031–1035. [[CrossRef](#)]
30. Sanyang, M.L.; Sapuan, S.M.; Jawaid, M.; Ishak, M.R.; Sahari, J. Effect of glycerol and sorbitol plasticizers on physical and thermal properties of sugar palm starch based films. In Proceedings of the 13th International Conference on Environment, Ecosystems and Development (EED ‘15), Kuala Lumpur, Malaysia, 23–25 April 2015; p. 157.
31. Nunes, C.; Mahendrasingam, A.; Suryanarayanan, R. Investigation of the multi-step dehydration reaction of theophylline monohydrate using 2-dimensional powder X-ray diffractometry. *Pharm. Res.* **2006**, *23*, 2393–2404. [[CrossRef](#)] [[PubMed](#)]
32. Asada, M.; Takahashi, H.; Okamoto, H.; Tanino, H.; Danjo, K. Theophylline particle design using chitosan by the spray drying. *Int. J. Pharm.* **2004**, *270*, 167–174. [[CrossRef](#)]
33. Huanbutta, K.; Terada, K.; Sriamornsak, P.; Nunthanid, J. Simultaneous X-ray Diffraction-Differential Scanning Calorimetry and Physicochemical Characterizations of Spray Dried Drugs and Chitosan Microspheres. *Walailak J. Sci. Technol.* **2016**, *13*, 849–861.
34. Huanbutta, K.; Sangnim, T.; Sittikijyothin, W. Physicochemical characterization of gum from tamarind seed: Potential for pharmaceutical application. *Asian J. Pharm. Sci.* **2016**, *11*. [[CrossRef](#)]
35. Kesavan, J.G.; Peck, G.E. Solid-state stability of theophylline anhydrous in theophylline anhydrous-polyvinylpyrrolidone physical mixtures. *Drug Dev. Ind. Pharm.* **1996**, *22*, 189–199. [[CrossRef](#)]
36. Aguilar, J.E.; Montoya, E.G.; Lozano, P.P.; Negre, J.M.S.; Carmona, M.M.; Grau, J.R.T. New sedem-odt expert system: An expert system for formulation of orodispersible tablets obtained by direct compression. In *Formulation Tools for Pharmaceutical Development*; Elsevier: Amsterdam, The Netherlands, 2013; pp. 137–154.
37. Ruiz-Picazo, A.; Colón-Useche, S.; Gonzalez-Alvarez, M.; Gonzalez-Alvarez, I.; Bermejo, M.; Langguth, P. Effect of thickener on disintegration, dissolution and permeability of common drug products for elderly patients. *Eur. J. Pharm. Biopharm.* **2020**, *153*, 168–176. [[CrossRef](#)]
38. Castro, P.M.; Sousa, F.; Magalhães, R.; Ruiz-Henestrosa, V.M.P.; Pilosof, A.M.; Madureira, A.R.; Sarmiento, B.; Pintado, M.E. Incorporation of beads into oral films for buccal and oral delivery of bioactive molecules. *Carbohydr. Polym.* **2018**, *194*, 411–421. [[CrossRef](#)] [[PubMed](#)]